

EMBRY-RIDDLE

Aeronautical University™

SCHOLARLY COMMONS

Dissertations and Theses

2012

Ranging of Aircraft Using Wide-baseline Stereopsis

Kevin Todd Rigby

Embry-Riddle Aeronautical University - Daytona Beach

Follow this and additional works at: <https://commons.erau.edu/edt>



Part of the [Aviation Commons](#), and the [Mechanical Engineering Commons](#)

Scholarly Commons Citation

Rigby, Kevin Todd, "Ranging of Aircraft Using Wide-baseline Stereopsis" (2012). *Dissertations and Theses*. 119.

<https://commons.erau.edu/edt/119>

This Thesis - Open Access is brought to you for free and open access by Scholarly Commons. It has been accepted for inclusion in Dissertations and Theses by an authorized administrator of Scholarly Commons. For more information, please contact commons@erau.edu.

Ranging of Aircraft Using Wide-baseline Stereopsis

By

Kevin Todd Rigby

Ed.D., University of West Florida, 2010

M.A.S., Embry-Riddle Aeronautical University, 1999

B.S., University of Central Florida, 1995

A thesis submitted to the Department of Mechanical Engineering
College of Engineering
Embry-Riddle Aeronautical University
In partial fulfillment of the requirements for the degree of
Master of Science in Mechanical Engineering

2012

© 2012 Kevin Todd Rigby


Ranging of Aircraft Using Wide-baseline Stereopsis

by


Kevin Todd Rigby

This thesis was prepared under the direction of the candidate's thesis committee chairman, Charles F. Reinholtz, Department of Mechanical Engineering, and has been approved by the members of his thesis committee. It was submitted to the Mechanical Engineering Department and was accepted in partial fulfillment of the requirements for the degree of Master of Science in Mechanical Engineering.


THESIS COMMITTEE:



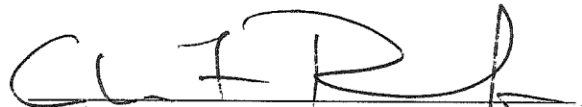
Charles F. Reinholtz, Ph.D.
Committee Chair



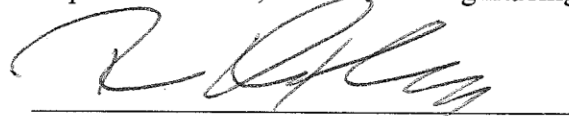
Timothy A. Wilson, Sc.D.
Committee Member



Shawn M. Doherty, Ph.D.
Committee Member



Charles F. Reinholtz, Ph.D.
Department Chair, Mechanical Engineering



Robert M. Oxley, Ph.D.
Associate VP for Academics

Acknowledgements

I would like to take this opportunity to thank my committee, Dr. Charles Reinholtz (Chair), and Dr. Tim Wilson and Dr. Shawn Doherty (committee members), for the encouragement and support throughout the dissertation process. Their feedback and guidance were incredibly valuable.

Thanks to Dr. Dan Macchiarella, my department chair at Embry-Riddle, who supported me by allowing me the opportunity to attend courses. He also allowed me the time to focus on completion of the thesis.

I would like to thank my parents, Kenneth and Sharon Rigby, for raising me to always strive for excellence. Their lessons have always served me well.

Finally, most of all I would like to thank Cindy, my wife of 24 years, and my children, Danielle and Brandon. Cindy has stood behind me in all of my endeavors. Her love, time, and devotion to me, our home, and our family have always been a key part of my successes. Thanks to my children for the sacrifice of time not spent with their father.

Table of Contents

Acknowledgments.....	iv
List of Tables	ix
List of Figures.....	x
Abstract.....	xi
Chapter I.	
Introduction.....	1
A. Theoretical Framework.....	3
B. Baseline.....	4
C. Statement of the Problem	4
D. Research Questions	5
E. Method	6
F. Significance of the Study.....	6
G. Chapter Summary	6
Chapter II.	
Review of the Literature.....	7
A. Introduction	7
B. Operational Aspects of Unmanned Aerial Systems	7
C. Visual Operation.....	8
D. Human Sensing.....	8
E. Visual Sensing.....	9
1. Rods and cones.....	9
2. Perceiving visual space	10
3. Oculomotor cues	11
4. Pictorial cues.....	11
5. Movement-produced cues.....	12
7. Motion Processing	13
8. Binocular disparity.....	13
9. Environmental variables affecting pilots	15
10. Summary	17
F. Intelligent Machines.....	17
1. Remote control	18
2. Teleoperation	18

3. Telepresence	19
4. Semi-autonomy	19
5. Autonomy.....	19
G. Robotic Sensing	20
1. Proprioceptive sensing	20
2. Exteroceptive sensing	20
H. Light-based Sensing	22
1. Light stripers	22
2. Laser range finders.....	22
3. Stereo camera pairs.....	23
I. Computer Vision.....	24
1. Charge coupled devices.....	24
2. Images.....	25
3. Camera parameters.....	25
4. Intrinsic camera error.....	25
a. CCD noise	25
b. Pixel hot spots	25
c. Blooming	26
d. CCD alignment	26
f. Distortion	27
5. Extrinsic camera error	27
J. Stereopsis.....	28
1. Vergence versus parallel images.....	28
2. Disparity range	28
a. Minimum disparity range	30
b. Maximum disparity range.....	30
K. Disparity Error	31
L. Correspondence problem.....	31
M. Chapter Summary	32

Chapter III.

Method	33
A. Introduction	33
B. Research Design	33
C. Samples.....	33
1. Human ranging pilot study	33
2. Stereo ranging study	33
D. Research Questions and Hypothesis	34
E. Variables	34
1. Human ranging pilot study	35
a. Dependent variable 1.....	35

	b. Dependent variable 2.....	35
	2. Stereo ranging study	35
	a. Independent variable 1	35
	b. Independent variable 2.....	36
	c. Dependent variable.....	36
F.	Procedure	36
	1. Human ranging pilot study	36
	a. Location setup.....	36
	b. Data collection	36
	2. Stereo range study.....	37
	a. Camera setup.....	37
	b. Camera calibration	38
	c. Camera alignment.....	38
	d. Data collection	40
	3. Data analysis.....	41
	a. ADS-B data analysis	42
	b. Stereo image pair analysis.....	42
	c. Hypothesis 1 analysis.....	42
	d. Hypothesis 2 analysis.....	43
	e. Hypothesis 3 analysis.....	43
G.	Chapter Summary	43
Chapter IV	Results	44
	A. Introduction	44
	B. Research Questions	44
	C. Ranging Results	44
	1. Human ranging pilot study	45
	2. Stereo study data	45
	D. Data Analysis	46
	1. Research question 1	46
	2. Research question 2	46
	3. Research question 3	47
	E. Chapter Summary	47
Chapter V	Conclusions.....	48
	A. Introduction	48
	B. Study Summary.....	48
	C. Results.....	48
	1. Research question 1	49
	2. Research question 2	49

3. Research question 3	49
D. Discussion.....	50
1. Research question 1	50
2. Research question 2	50
3. Research question 3	50
E. Implications of the Study.....	50
F. Recommendations for Future Research.....	51
G. Limitations of the Study	52
H. Aircraft Deployment	52
I. Chapter Summary	53
References	54
Appendixes.....	57
A. Examples of Aircraft Image Pairs	58
B. File Usage Evaluation Criteria.....	61
C. Human Ranging Pilot Study Data	63
D. Stereo Ranging Study Data	65

List of Tables

1. Human Ranging Pilot Study Descriptive Data	45
2. Wide-based Stereo Descriptive Data	46

List of Figures

1. Narrow-baseline disparity.....	14
2. Relative disparity at 1 and 5 meters	15
3. Display of variables for the calculation of disparity range	29
4. Stereo camera setup used in the research study	38
5. Initial camera alignment method	39
6. Manual verification calibration fixture	40
7. Example stereo dataset.....	42

Abstract

Ranging of Aircraft Using Wide-baseline Stereopsis

Kevin Todd Rigby

The purpose of this research was to investigate the efficacy of wide-baseline stereopsis as a method of ranging aircraft, specifically as a possible sense-and-avoid solution in Unmanned Aerial Systems. Two studies were performed: the first was an experimental pilot study to examine the ability of humans to range in-flight aircraft and the second a wide-baseline study of stereopsis to range in-flight aircraft using a baseline 14.32 meters and two 640 x 480 pixel charge coupled device camera. An experimental research design was used in both studies. Humans in the pilot study ranged aircraft with a mean absolute error of 50.34%. The wide-baseline stereo system ranged aircraft within 2 kilometers with a mean absolute error of 17.62%. A t-test was performed and there was a significant difference between the mean absolute error of the humans in the pilot study and the wide-baseline stereo system. The results suggest that the wide-baseline system is more consistent as well as more accurate than humans.

Chapter I

Introduction

Unmanned systems are becoming more prevalent in our society, in the military, and in industry. Unmanned Aerial Systems (UAS) are commonplace in military operations. Limited commercial operations are allowed in the National Airspace System (NAS) on a case-by-case basis. One of the current Federal Aviation Administration (FAA) requirements placed on UAS operators in the NAS is sense-and avoid capability (FAA, 2008). Humans and robots can sense using multiple complex systems. This study was on one aspect, vision, as a potential solution to the sense and avoid problem.

A pilot flying a manned aircraft uses several methods to sense-and-avoid other aircraft. In reference to the sense-and-avoid principal, “A frequently asked question in human factors engineering is whether the role assigned to the human being is within his or her capabilities” (Liebowitz, 1988, p. 85). In both radar and non-radar environments visual scanning is the primary method used by pilots. Pilots must pick aircraft out of the visual field and determine whether an aircraft is a threat. Initial threat determination is based on whether or not the aircraft is on a collision course with the pilot’s aircraft. Final threat determination is based on direction and velocity. Humans range objects using a combination of visual cues to include oculomotor cues (heuristic feelings in eye muscles, not possible beyond about 3 meters), pictorial cues (a pilot sees and identifies a Cessna 172), movement cues (a Cessna 172 moves across a visual field at an estimable rate), and

binocular disparity (the differences in scene between the left and right eye)(Goldstein, 1999).

There are three types of UAS operations: teleoperation, semi-autonomous, and autonomous. Teleoperation is when a human operator controls a robot beyond visual range using sensing information such as flight instruments and a video feed. Semi-autonomous operation or supervisory control is where the robot is given a portion of a task that it can safely do on its own. An example of this would be when a pilot places a UAS on autopilot, but is still monitoring the aircraft at all times, such as with a Global Hawk UAS. Autonomous control would be required when an aircraft is out of communication with ground-based control (Murphy, 2000).

One issue with teleoperation is limited information (Murphy, 2000). In a teleoperated vehicle, video cameras supply a limited field of view. Computer monitors also produce eyestrain and fatigue (Blehm, Vishnu, Khattak, Mitra, & Yee, 2005). The same will occur when monitoring a semi-autonomous vehicle. This fatigue and boredom may result in missing a visual cue and detecting an aircraft. An autonomous vehicle must sense and avoid aircraft without the use of an operator monitoring visual systems. These issues make computer vision systems a possible candidate for addressing the sense and avoid issue in UAS operations.

Computer vision is based on processing data from any sensor which uses the electromagnetic spectrum and produces a recognizable image (Murphy, 2000). A reactive computer vision system will consist of one or more cameras. Most reactive robots use charged coupled device (CCD) cameras (Murphy, 2000). CCD cameras are capable of producing a matrix structure of an image (Klinger, 2003). The benefit is that matrices are

computationally tractable using a computer. Using an algorithm, a decision can be made about data.

One could propose any three of the four methods that humans use to range objects for use in reactive robotic systems. Oculomotor cues are heuristic in nature to the physiology of the human eye. Pictorial and movement cues require in depth artificial intelligence (AI) algorithms that require heavy processing power. The fourth method, binocular disparity falls under the category of stereopsis in both human and computer vision (Forsythe & Ponce, 2003).

Theoretical Framework

This study investigates the efficacy of using stereopsis for ranging aircraft. Common methods in stereopsis were used to complete the study. The study was a structured exploration of using wide-baseline stereopsis.

Ranging in reactive robots can be accomplished using three types of vision systems: light stripers, laser range finders, and stereo camera pairs (Murphy, 2000). Light stripers and laser range finders are used to scan surfaces and develop image maps. Stereo vision camera systems are capable of taking in an entire visual field.

Stereopsis is theoretically unlimited in range. A specific stereo camera system will be limited in range based on two factors: camera parameters and camera baseline. Camera parameters are focal length and CCD pixel size. Camera baseline is how far apart the two cameras are placed. The limitations of the camera using the three variables of focal length, pixel size, and baseline will result in a minimum and maximum disparity ranges for the stereo camera systems (Ahuja, 2009). Disparity is the distance in the location of the point of interest between two stereo camera images (Murphy, 2000).

Maximum disparity range would occur at a point where there is no discernible difference in the change in range over time a significant distance. Disparity range would be met for example if the image moves, but beyond the maximum range it still remains within the same pixel in the image matrix.

Baseline

It is not uncommon to find stereo camera systems in use on reactive robotic vehicles. High quality stereo camera systems are readily available for acquisition. However, these systems are typically on a narrow-baseline of just a few inches. The requirement for the robots for which these camera systems would be used would be for the application of a robot that would not have to sense accurately beyond a few meters. For the purposes of this study, a narrow baseline will be considered any baseline less than 3 meters, which would be about the width of the widest road vehicle.

Baseline is typically set by determining the maximum disparity error allowable in a given application. Widening baseline will reduce disparity error. The trade-off is that widening the baseline increases the minimum disparity range. Minimum disparity range is a function of focal length. Minimum disparity range is where the two fields of view of the camera do not overlap between the two cameras in the foreground. The far field is of greater concern in sense-and-avoid, therefore the increase in minimum disparity range is not a factor. A wide-baseline would be suitable for increasing the disparity range and make stereopsis a candidate for ranging of aircraft.

Statement of the Problem

Unmanned Aerial Systems require sense and avoid capabilities for operation in the NAS. Below 10,000 feet in the NAS, aircraft are limited to 250 knots indicated

airspeed (KIAS). At 250 KIAS, the closing rate is such that aircraft within 5 nautical miles (3.125 kilometers) of one another are considered a possible threat to one another. In terms of sense-and-avoid, if pilots can spot an aircraft in their visual field, they can then begin to determine threat by determining range.

Many manned aircraft carry transponders. However, many do not and are not required to by Federal Aviation Regulation (FAR). Systems like Terminal Collision Avoidance Systems (TCAS) and Automated Dependent Surveillance – Broadcast (ADS-B) technologies are common in many new aircraft. However, they depend on other aircraft having transponders of one type or another. The threat of collision with a UAS is based on aircraft without transponders. These aircraft by FAR would be operating in Visual Meteorological Conditions (VMC). Therefore, human see-and-avoid is the primary method of collision avoidance. A UAS fitted with an automated see and avoid system would be ideal as a primary system for an autonomous UAS, and as backup for a teleoperated or semi-autonomous UAS. Wide-baseline stereopsis may be a suitable candidate as a base for a UAS visual sense-and-avoid system.

Research Questions

Based on the theoretical framework, three research questions were developed:

1. Can a wide-baseline stereo camera pair range an in-flight aircraft?
2. Can a wide-baseline Axis[®] 207W 640 x 480 pixel stereo camera pair range an in-flight aircraft beyond 4.8 kilometers using a baseline of 14.32 meters?
3. Can a wide-baseline stereo camera pair range in-flight aircraft more consistently than the sample of humans used in the human ranging pilot study?

Method

The research design in this study was a quantitative experimental method. The study was performed at Embry-Riddle Aeronautical University (ERAU). This study used a wide-baseline stereo camera system placed on top of one of the university buildings. The stereo camera system was used to take pictures of aircraft within 10 kilometers. Simple triangulation based on disparity between two images was used to estimate the distance to the aircraft. ADS-B data was used to determine the actual position of the aircraft. The differences between the estimated and actual position were determined and were used for analysis.

Significance of the Study

The efficacy of wide-baseline stereopsis was tested. The results will be discussed in Chapter 4. The potential use of wide-baseline stereopsis has the potential to contribute to the sense-and-avoid problem for UAS. This study is significant in the fact that it provides research data on ranging of aircraft using wide-baseline stereopsis. The data may be used to carry forward with future research based on the results.

Chapter Summary

A background of the use of stereopsis was discussed in this chapter. A theoretical foundation based on common methods in stereopsis to propose the potential strength of wide-baseline stereopsis for the ranging of aircraft was presented. A method for testing the efficacy of wide-baseline stereopsis was also presented.

Chapter II

Review of Literature

Introduction

This chapter provides a review of the literature on using wide-baseline stereopsis for the ranging of aircraft. Operational aspects of Unmanned Aircraft Systems (UAS) will be discussed. Human visual sensing will be discussed with a focus on how manned aircraft crews sense-and-avoid other aircraft. The types, purposes, and roles of computer vision with a focus on stereopsis for the ranging of objects will also be discussed.

Operational Aspects of Unmanned Aircraft Systems

The current operational consideration of UAS in the National Airspace System (NAS) are allowed on a case-by-case basis. The approval to operate in the NAS in other than active Restricted, Prohibited, or Warning Areas, or in Class A airspace will be based on a Certificate of Authorization (COA) issued by the Federal Aviation Administration (FAA) under UAS Interim Operation Approval Guidance 08-01 (FAA, 2008). FAA approval of a COA is primarily concerned with the “applicant’s responsibility to demonstrate that injury to persons or property along the flight path is extremely improbable” (FAA, 2008, p. 8).

Many of the commercial UAVs are available with sensor suites that include a variety of onboard sensors. These sensors include lasers, radar, various cameras, and sonar. They are also available with integrated systems such as Terminal Collision

Avoidance Systems (TCAS) and Automated Dependent Surveillance Broadcast (ADS-B) for detection and avoidance of aircraft with certain types of transponders.

The FAA is concerned with the two types of targets, cooperative and non-cooperative. Cooperative targets are those with certain types of transponders that work actively with TCAS and ADS-B. Cooperative targets are easily recognizable and TCAS will issue alerts and resolution advisories to pilots to avoid collision.

Non-cooperative targets are those without transponders. These include balloons, gliders, ultra-light, and light aircraft. These targets also present low radar reflectivity as primary radar targets (FAA, 2008).

Visual Observation

Visual observation is important to UAS operations for the purpose of sense and avoidance of other aircraft. UAS operations outside of Restricted, Prohibited, or Warning Areas, or Class A airspace are required to have visual observers that are either airborne or ground-bases (FAA, 2008). Applicants proposing “see-and-avoid” strategies, in lieu of visual observers, need to support proposed mitigations with safety studies which indicate the operations can be conducted safely.

Properly prepared computers do not fatigue in the way that humans fatigue. Given enough processing power, their attention is not divided among other tasks, such as would be the case with a human operator. Computer vision is an ideal candidate as part of a sense-and-avoid system.

Human Sensing

Humans use a variety of sensors to perceive the environment surrounding them and then recognize patterns that will produce a behavior. Behavior can be action or

inaction. Human senses include visual (seeing), vestibular (inner ear), aural (hearing), taste, olfactory (smell), and tactile (touch). These senses are often combined into systems such as the somatosensory system, for example, which includes proprioception (the sense of position of the limbs) and kinesthesia (the sense of movement of the limbs) (Goldstein, 1999). The somatosensory system combines visual, vestibular, and kinesthetic sensors to achieve perception.

Humans use two senses for ranging of objects: aural and visual. For aural sensing, binaural cues (the differences between the left and right ear) result in interaural differences. Interaural time differences for example will give a cue of direction. Since pilots would be in an aircraft that interferes with these aural cues, aural ranging is not a variable in this study. This means that for detection and ranging of aircraft 100 % of human sensing of in-flight aircraft will result from visual cues.

Visual Sensing

Human visual sensing is based on the reception of visible light on the retina. Humans perceive visible light in the electromagnetic radiation spectrum in the range 380 to 760 nanometers in wavelength (DeHart, 1985). The retina is made up of an optical array of rod and cone shaped receptors. Photons excite the rods and cones and produce a stimulus. This stimulus is the result of light being transduced into electricity, a signal which is carried to the brain through the cerebral cortex. The pattern produced by the stimulus on the optical array results in a perceptual cue (Goldstein, 1999).

Rods and cones. The distribution of rods and cones in the eye is not even. The highest density of cones occurs near the center of the retina in an area about the size of this small letter “o” in a size 10 font (Goldstein, 1999). The fovea is the point of central

focus of light through the lens of the eye. Outward from the fovea the distribution of rods and cones changes exponentially. Overall, the retina contains far more rods than cones, about 120 million rods and 6 million cones (Goldstein, 1999).

Rods are more sensitive to shorter wavelengths than cones. Cones receive peak light at a wavelength of 555 nanometers in the yellow-green spectrum. At about 510 nanometers rods begin to receive more light than cones and peak at around 490 nanometers in the blue-green spectrum. These differences in light causes differences in visual acuity as light changes. Visual acuity is highest in the cone rich fovea in bright light and shift to the rods as light diminishes until all luminosity is gone (DeHart, 1985). Based on this discussion, rods are more sensitive to light than cones due to the fact that they require less light. This means that movement of an object is more likely to be detected by the rods. This results in peripheral vision being more sensitive to movement. However, the cones are more sensitive to detail. Therefore, if fine movement is detected it must be targeted and directly viewed in the visual field. Direct viewing becomes more difficult as the light intensity drops.

Perceiving visual space. Humans perceive visual space using a combination of depth cues. “The *cues* approach to depth perception focuses on identifying information in the retinal image that is correlated with depth in the scene” (Goldstein, 1999, p. 215). There are two basic types of visual cues: oculomotor and visual. Oculomotor cues are cues which are kinesthetic. Visual cues are produced by the scene played out on the retina and are subdivided into monocular and binocular cues. Monocular cues include pictorial and movement-produced cues. Binocular cues are based in stereopsis (Goldstein, 1999; Blake & Sekuler, 2006).

Oculomotor cues. Oculomotor cues are based on a human's ability to sense the position of our eyes and the tension in eye muscles. These cues are based on basic feelings in the eyes that occur from two sources, the eye muscles that move the eyes and from the movement of the lens of the eye. Convergence occurs when the eyes target something close to the face and the eyes cross producing tension in the muscles of the eyes. This is a cue that the object is near. Accommodation occurs when the lens of the eye changes shape and bulges to focus on an object near the face (Goldstein, 1999; Blake & Sekuler, 2006). Oculomotor cues are only reliable at a distance of about 1 to 3 meters and are not reliable cues in the detection of distant objects such as in-flight aircraft.

Pictorial cues. Pictorial cues are static depth cues that can be depicted in a painting by an artist or in a photograph (Goldstein, 1999; Gibb, Gray, & Scharff, 2010). Making sense of pictorial cues is heuristic in nature, meaning that the observer must be able to identify objects in a scene and have some prior knowledge about those objects. Pictorial cues include: occlusion, atmospheric perspective, relative height, familiar size, linear perspective, texture gradient, and shadows. (Goldstein 1999; Gib et al., 2010).

Take for example, a flatland that leads to distant mountains. An occlusion would occur if one mountain partially hides another and an observer would know that the occluded mountain is farther away. If the sky were clear then an observer would be able to see more detail and the atmosphere would have an effect that would make the mountain seem to be nearer than if it were hazy (atmospheric perspective). If the mountain were near and the peak above the observer, then the object would appear higher in the visual scene and a sense of height would be gained (relative height). If a car were on the side of the mountain on a road, a sense of familiar size would be gained. If a

straight road led to the mountain, and the lines of the road disappeared into the distance, then a sense of linear perspective would be gained. If a series of equally farmed fields were next to the road in the valley, and led up to the mountain, then a texture gradient would be evident, and the farther fields would appear smaller. If the sun were setting behind the mountains, then shadows would begin to fall in front of the mountain and provide more linear perspective. Using all of these pictorial cues an observer could make an estimation of range.

A pilot attempting to determine the range of an aircraft might use any of these visual cues to estimate range. The primary cue that may affect range estimation is atmospheric perspective, especially if there are no other visual cues in the sky. Haze in the atmosphere would reduce the visible detail of an aircraft. This might make the aircraft unrecognizable or seem slightly smaller. The pilot would merely know that an object is in the distant sky and range determination would be highly unreliable.

Movement-produced cues. An observer may move and the observed object may move. These movements produce two movement cues, motion parallax and deletion/accretion. Motion parallax is produced by the appearance of near or far objects appearing to move at relatively different rates across the visual field. Deletion/accretion occurs when two objects overlap and movement covers (deletion) or uncovers (accretion) the object which is more distant. Deletion/accretion is related to motion parallax in that the overlapping surfaces appear to move relative to one another. Deletion/accretion is related to the pictorial cue of occlusion (Gibb et al, 2010). An object that moves faster in the visual field will appear nearer than an object that moves slower. (Goldstein, 1999; Gibb et al., 2010).

Take for example a driver speeding down a road in an open field who enters a segment of road lined with evenly spaced trees. The trees in the distance will appear to move more slowly than the trees that are near due to motion parallax. Accretion is also occurring as distant trees are uncovered. Depending on where the driver looks, his/her sense of speed will change. If the driver enters another segment of road where the trees are at twice the distance from the road, then a variable in the motion cue has changed and the driver may experience a difference in perceived distance. Other variables that would affect the perceived cue might be the type, size, and spacing of the trees. Atmospheric perspective will also affect motion parallax by reducing the detail of the trees making them appear smaller and spaced further apart..

Motion processing. The object moving in the visual field will cause a local shift of an image on the retina. An observer moving the eyes or the body will cause an entire shift of the visual image on the retina. “Expansion, contraction, and rotation of the entire visual field are all components of *optical flow* information” (Gibb et al., 2010, p. 45). Optical flow is another term for motion parallax (Davis, Johnson, Stepanek, & Fogarty, 2008).

Binocular disparity. Stereoscopic vision is based in binocular disparity. “Stereoscopic vision involves combining the images from the two eyes in order to judge the depth of objects in one’s environment” (Gibb et al., 2010). Binocular disparity is based on the differences between the scenes presented to the optical matrix of the retina. Retinal disparity is the difference between the location of an object on a given plane in the two separate scenes, or images (Blake & Sekuler, 2006). The appearance of the model aircraft in Figure 1 is an example of disparity between a left and right camera image at a

range of approximately 1 meter and a baseline of approximately 0.1 meters.

In essence, each eye gives a different viewpoint of a viewed object (Goldstein, 1999). Simply closing one's eyes alternately, while focusing on an object, will create the effect.



Figure 1. Narrow base-line disparity. Copyright 2012 by Kevin Todd Rigby.

The magnitude of disparity is a function of how far away the object is and how far apart the eyes are located. Binocular disparity (δ) is related to depth (ΔD), interocular separation (I), and distance (D) as seen in Equation 1 (Gib et al.):

$$\delta \approx I \Delta D / D^2 \quad (1)$$

Binocular disparity will change with the square of the distance and become very small as distance increases. In humans, interocular separation can be assumed at approximately 65 millimeters and will not vary more than a few millimeters in a normal adult (Hibbard, 2008).

Rearranging Equation 1 results in Equation 2:

$$\Delta D = \delta D^2 / I \quad (2)$$

Figure 2 is an example of how distance affects the relative disparity of an object when viewed from 1 and 5 meters on a 0.065 meter baseline from an Olympus FE-230 point

and shoot CCD camera.

As distance increases to very large ranges such as between two aircraft, small changes in disparity serve as a poor cue for depth perception and it is assumed that pilots will rely primarily on monocular cues (Gibb et al., 2010). According to Goldstein (1999), binocular disparity cues become unreliable at about 30 meters.

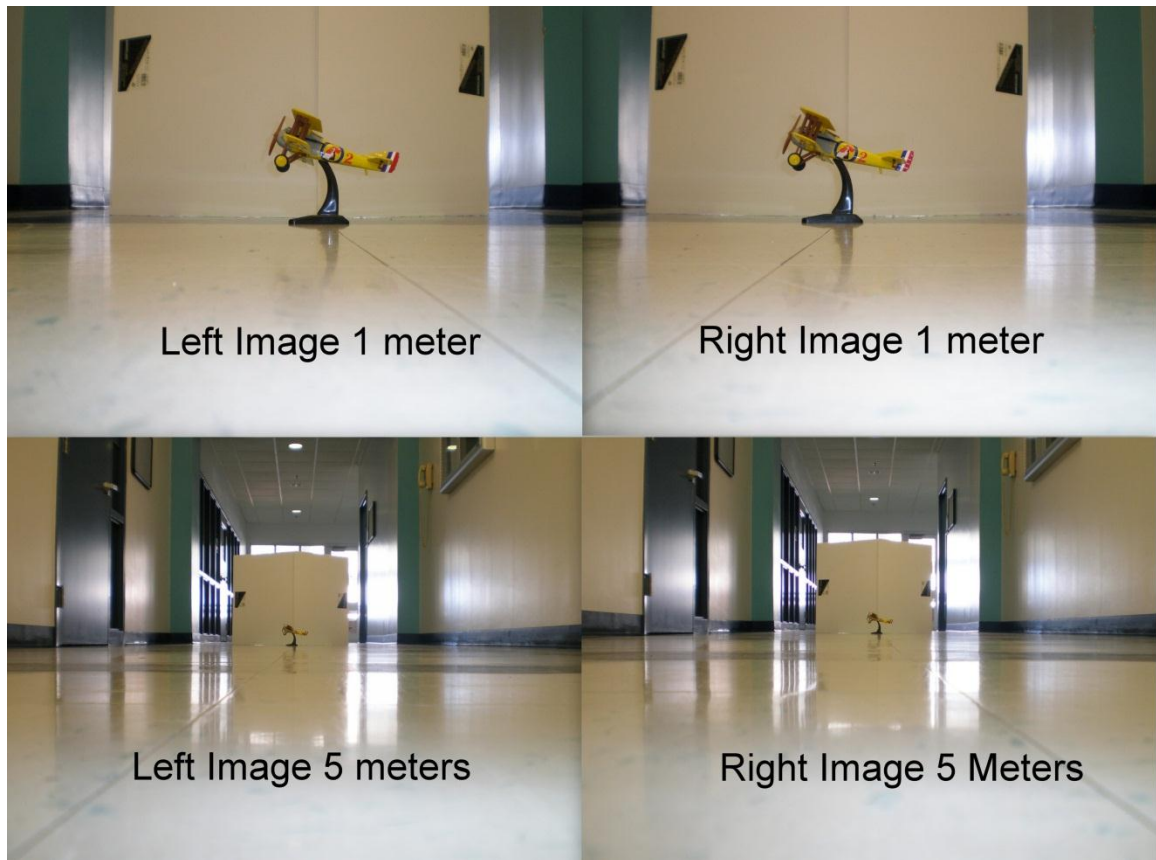


Figure 2. Relative disparity at 1 and 5 meters using a human equivalent baseline of 0.065 meters. Copyright 2012 by Kevin Todd Rigby.

Environmental variables affecting pilots. Atmospheric perspective and low luminosity have already been discussed as environmental variables that can affect the variability of depth perception in humans. Environmental variables that specifically affect pilots include vibration, hypoxia, visual acuity, and contaminated windscreens.

Vibration directly affects the lens of the eye. A large range of vibrations are transmissible to the pilot in an aircraft (Dehart & Davis, 2002). “Difficulties in reading instruments and performing visual searches occur when vibrations introduce relative movement of the eye with respect to the observed object or target” (DeHart & Davis, 2002, p. 165).

Hypoxic (altitude) hypoxia occurs in pilots as altitude is increased. As altitude increases, the density of the air humans breathe decreases. Therefore, the amount of oxygen per breath decreases. This reduction of oxygen results in lower blood oxygenation, and has adverse effects in humans. The symptoms of hypoxic hypoxia become evident after about 5,000 feet above mean sea level (Reinhart, 2008). “Vision is the first of the special senses to be altered by a lack of oxygen, as evidenced by diminished night vision” (DeHart & Davis, 2002, p. 368).

In private pilots, visual acuity would serve as a variable in visual sensing. Private pilots are required by the FAA to hold a 3rd Class medical certificate. Vision requirement to obtain the 3rd Class medical certificate is 20/40 or better visual acuity in each eye with or without correction (FAA, 2010). Visual acuity is how sharp or crisp an object will appear to be at a given distance. Normal visual acuity is 20/20 and is tested for example by a subject being able to read a given line of letters on a chart at 6 meters distance (DeHart, 1985). Anything greater than 20/20, 20/40 for example, means that the subject will not have the same clarity of a visual image as a person with 20/20 visual acuity. This difference in visual acuity will affect the variability of depth perception in the same way as atmospheric perspective by reducing detail and reliability of pictorial cues. A film of dirt on a windscreen might have a similar effect.

Summary. Humans visually sense based on the reception of visible light. Visual space is perceived based on several depth cues to include both monocular and binocular cues. At ranges beyond about 30 meters binocular cues become unreliable and monocular cues are primary for depth perception. Visual sensing reliability diminishes as environmental factors involved in aviation are considered. For the purpose of this research, the best case scenario for perceiving visual space would be a person standing on the ground at sea level near noon on a clear day. The worst case scenario would be a private pilot with 20/40 visual acuity in an aircraft with high vibration and a dirty windscreen flying at sunrise or sunset above 5,000 feet mean sea level.

The best case scenario will be considered for this research as it would be the minimum error encountered. A pilot study of human ranging of aircraft was performed by the researcher and a student assistant and suggests that humans have a large percent error when ranging in-flight aircraft (See Chapters 3 and 4). The only variable not accounted for in the pilot study on human ranging was that of acuity.

Intelligent Machines

The idea of man-made machines functioning autonomously dates back centuries. Hephaestus fashioned girls from gold to help him with his work in the *Iliad*. The term automata was used for centuries to describe automated machines, such as Jacques Vaucanson's 1738 mechanical copper duck which ate, drank, bathed, and quacked autonomously. In the 1920s Karel Capek wrote a play titled *Rossum's Universal Robots*. The name of the manufacturer, Rossum was taken from the Czech word rozum which means reasoning. The name for the play's humanoid automata was taken from the Czech word robota which means worker. The central theme of the story was reasoning universal

robots, or intelligent machines, which could work for the creation of a better world for humans. In the end, the robots destroyed humanity and made a better world for themselves instead. The play became popular, and the word robot became the coined phrase replacing automata in society (Asimov & Frenkel, 1985).

Intelligence is required to operate autonomously. Intelligence in humans is gathered through the senses and processed in the brain. “An intelligent robot is a mechanical creature which can function autonomously” (Murphy, 2000, p. 3). Niku (2001) classifies an intelligent robot as “a robot with the means to understand its environment and the ability to successfully complete a task despite changes in the surrounding conditions under which it is to be performed” (p. 2). An intelligent robot would gather information through sensors and process that information through a central computer. The robot would then use an algorithm to produce a behavior of action or inaction. Murphy (2000) calls this application of science and engineering to make machine act intelligently *artificial intelligence* (AI).

Robots can be classified into two categories: human operated and autonomous. Human operated robots can be remotely operated or semi-autonomous. Remotely operated robots include remote, teleoperated, and telepresence controlled (Murphy, 2000).

Remote control. Remote control is where the operator sees the robot and controls the robot in visual range. An example of this type of robot would be a robotic manipulator arm. Or, it could be as simple as a remote control toy car.

Teleoperation. Teleoperation is where the operator sees instruments on a control panel and controls a robot in or out of visual range. These instruments may include video

and telemetry data. An example of a teleoperated robot would be a Predator MQ-1 UAS. The MQ-1 is a 48 foot wingspan high-altitude surveillance UAS that can be operated out of line of site (LOS) and maintain its station for a period of over 24 hours. The MQ-1 is operated from a ground control station (GCS) by teleoperation either LOS radio or out of LOS satellite. The pilot of this vehicle would utilize a video and flight instrumentation data from the aircraft for takeoff, landing, and operation of the aircraft.

Telepresence. A robot operated through telepresence would be one that is controlled through the operator seeing and feeling the environment through feedback sensors. An example of telepresence is the world's first telerobotic surgery performed on a patient in Strasbourg, France from New York, New York on September 7, 2001 which involved the removal of the patient's gallbladder (Anvari, McKinley, and Stein, 2005). In this case, the surgeon would use up to three manipulators: one to lift the gallbladder and hold it, one to cut away the gallbladder, and one to see the area of operation.

Semi-autonomy. A semi-autonomous robot is one that can be directly controlled by a human operator, or it can be placed in autonomous mode and be monitored by the operator for certain pre-programmed tasks. The MQ-1 Predator also has semi-autonomous capabilities and can be placed on autopilot for all parts of a flight with the exception of takeoff or landing.

Autonomy. An autonomous robot would be one that would be released into an environment and no human monitoring would be required for it to complete its job. An example would be that of an autonomous ground vehicle such as those in the Defense Advanced Research Projects Agency (DARPA) Grand Challenge. The DARPA Grand Challenge vehicles were released into an environment and were required to navigate

safely through neighborhoods and simulated traffic while avoiding pedestrians without human intervention. These vehicles required a suite of sensors that could detect road edge lines and objects coupled with differential GPS.

Robotic Sensing

To achieve remote or autonomous operation, a robot must have a suite of sensors appropriate to the environment and task. “An artificially intelligent robot must have some sensing in order to be considered a true AI robot” (Murphy, 2000, p. 202). According to Murphy, robotic sensing can be separated into two categories: proprioceptive (internal position sensing) or exteroceptive (environmental sensing).

Proprioceptive sensing. Proprioceptive sensors give a robot a sense of movements in reference to an internal reference frame. This can be the movement of the robots appendages or the body of the robot (Murphy, 2000). An example of proprioceptive sensing would be a shaft encoder. A shaft encoder uses a disc that is calibrated and attached to the hub of a robot’s wheel. The encoder has graduated markings that are read by an infrared sensor called an encoder. Based on how many markings pass the encoder, the robot can calculate how many feet it has moved forward. Error in this instrument would be due to different surfaces that may cause slippage during acceleration or turns. Shaft encoders can be used on wheels or appendages.

A second example of proprioceptive sensing would be an inertial measurement unit (IMU) which uses accelerometers and gyroscopes to tell the position, acceleration, and velocity of the robot in reference to a starting point, or a known point along a route. IMUs can be as simple as three microelectromechanical (MEMs) accelerometers arranged in order of axis x , y , z , or it can be as complicated as a stabilized three-ring laser

gyro. Error in an IMU grows over time and must be reset to some known point during extended operation. Magnitude of error will depend on the quality of the IMU.

Exteroceptive sensing. Exteroceptive sensors give a robot the layout of objects in its environment and the location of objects around it. Exteroceptive sensors include both active and passive sensors. The difference between active and passive sensors is that active sensors produce their own source of excitation and passive devices receive only the signals that exist in the environment. Many active sensors can also be used as passive sensors if the source of excitation is turned off. However, a sensor must be sensitive enough to receive the passive signal and filter it from other signals.

Common active sensors used in robotics include radio detecting and ranging (RADAR), light detecting and ranging (LIDAR), sound navigation and ranging (SONAR), and infrared cameras. Passive sensors include RADAR, SONAR, Infrared Cameras, and Visible Light Cameras. Each of these have limitations on range depending on the medium in which they are transmitting. For the purpose of this study, the medium will be air in Earth's atmosphere.

Sound based systems such as ultrasonic sensing have a long cycle time in comparison to light-based systems. Sound based systems are also limited in range to about 3 meters and susceptible to specular reflection (Murphy, 2000). This makes sound based systems unsuitable for ranging of aircraft.

RADAR based systems have an equivalent time of flight to that of light-based sensing since both are near the speed of light in the Earth's atmosphere. However, RADAR based systems for ranging of aircraft as primary targets require very large power sources and can be assumed unsuitable for use on a small UAS since they are not even an

option for light civil aircraft. This leaves light-based systems. Light-based systems are relatively small and light weight and can be either active or passive. The relatively small size and weight make light-based systems a possible candidate for the ranging of non-participating aircraft.

Light-based Sensing

Light-based sensors use electromagnetic radiation (EMR) from the visible spectrum of light (380 to 760 nanometers in wavelength). Reactive robots can range their position in an environment and objects within that environment using three types of light-based vision systems: light stripers, laser range finders, and stereo camera pairs (Murphy, 2000).

Light stripers. Light stripers project light into an environment in the form of a grid pattern, dots, or line, and observe how the pattern is distorted in the image. The light is captured by a charged coupled device (CCD) camera and the structure of the light is compared to what it should be if it were projected at a given distance onto a flat surface. The difference between the actual image and the theoretical image are used in a processing unit to produce a map of the environment. Light stripers are used primarily for mapping rooms or obstacle avoidance (Murphy, 2000). A limitation of light stripers is brightly lit rooms. In a brightly lit room, light gets washed out and part of the image map is distorted or lost (Murphy, 2000). This limitation makes light striping unsuitable for aircraft ranging in bright sunlight.

Laser range finders. Laser range finders introduce light energy into the environment and use time of flight calculations to determine range. LIDAR uses this basic premise to map large areas. LIDAR accomplishes this by using a laser and mirror

on a rotating platform and takes a cross-sectional image of the environment. It then maps a series of cross-sectional images onto a CCD and is represented as an array which can then be processed into an image. “The range of a professional LIDAR device is around 100 to 200 meters, so it is effective both inside and outside” (Roble, 2005, p. 318). Airborne LIDAR systems for terrain mapping are typically limited to between 100 and 600 meters (Shan & Sampath, 2007). This limitation of range makes laser range finders unsuitable for aircraft ranging.

Stereo camera pairs. The use of stereo camera pairs to range an object is based on one of the same methods humans use to range objects, stereopsis. Disparity, or distance between the object in the x plane on two separate images is used to determine range using triangulation. Stereopsis is theoretically unlimited in range. A larger CCD matrix will theoretically increase the range of a stereo camera system.

The major drawback to extracting range from real-time camera systems is computational power. The typical range extraction algorithm for stereo mapping will require $O(n^2m^2)$ instructions (Murphy, 2000). Using Murphy’s estimation a 640 x 480 pixel CCD setup would require 9.43×10^{10} instructions to produce a single map. In comparison a 1280 x 960 pixel CCD would require 1.51×10^{12} instructions. Modern microprocessors can handle millions of instructions per second. Given an Intel® i7 processor that can handle 147,600 million instructions per second (MIPS), the two cameras would require 0.6389 and 10.23 seconds respectively to process a map.

The purpose of this research is not to map, but range a single object in the sky. Stereopsis has the potential to range aircraft. An in depth discussion of stereopsis follows

Computer Vision

Imaging systems can cover a broad range of integrated devices from early still-life film cameras, to medical ultrasound, to modern synthetic aperture radar, to radio telescopes. Imaging systems can use passive visible and non-visible light as well as electromagnetic radiation. Imaging systems can also be active and emit visible, infrared, and microwave radiation. If a sensor can detect a signal and a computer can use the signal to develop a profile, an integrated image can be displayed. The image can then be analyzed in some way.

CCDs, first proposed in 1970, have now replaced most cameras in modern applications, from hand held cameras and camcorders to special use cameras used in the sciences (Forsythe & Ponce, 2003). Machine vision systems use CCDs because of the fact that the image is captured as a matrix. The matrix can then be analyzed and post-processed by some mathematical algorithm. The output from the algorithm can then be used by the machine to perceive changes to its environment and produce a behavior. The following discussions and research are based on the use of CCD cameras. Therefore, a brief discussion on CCD cameras follows.

Charge coupled devices. Charge coupled devices are multi-layer semiconductor chips. CCDs are fabricated by building up a layer of silicon dioxide which is sensitive to photons of light in a given spectrum, and placing a conductive gate structure over the silicon dioxide. The gate structure serves as an array which undergoes manipulation by a positive charge that creates a potential at each gate. Electrons are then collected from each gate over a fixed period of time. The charge at each gate is analyzed and photo-conversion occurs (Forsythe & Ponce, 2003).

Images. Color images are produced by using filtered layers of semi-conductive material. For example, a CCD might have an array which has a top layer that filters red light, a middle layer that filters green light, and a final layer which receives the blue light. The multi-plane array can be expressed mathematically. After photo-conversion, a given pixel of (x, y) coordinate will have either a red-green-blue (RGB) or gray-scale bit value associated with it. For the purposes of image analysis the images are converted to a 256 bit gray-scale value, 0 being black and 255 being white.

Camera parameters. There are several camera parameters that affect computer vision. These include integration time, focal length, aperture type, lens type, and CCD size. These parameters affect image quality and error.

Intrinsic camera error. There are several possible intrinsic camera errors that include CCD Noise, CCD alignment, and distortion. When trying to range an object, CCD alignment and distortion errors can contribute to disparity error. Calibration and image rectification methods can be used to help reduce this error and will be discussed later.

CCD noise. CCD noise falls into four categories: fixed pattern noise (FPN), statistical noise, pixel hot spots, and blooming. The noise generated in a CCD is described by the signal to noise ratio (SNR) (Klinger, 2003).

FPN is the result of physical differences in CCD cells. “If all of the photoelements of the CCD cells were identical, the FNP would be zero” (Linger, 2003, p. 41). Statistical noise is generated by photons and electrons generated internally in the CCD, and noise generated in the output of the amplifier.

Pixel hot spots. Pixel hot spots are common in all CCDs. Pixel hot spots can be

observed by placing the camera in a sealed box and capturing images in the dark. The hot pixels will show up as white spots.

Blooming. Blooming is caused by the overflow of electrons into adjacent CCD cells. An area in an image with a strong light source, such as a laser pointing at the camera, will appear larger than its actual size. The edges will also appear to be smudged. CCDs can be designed with anti-blooming gates around the edges of each cell which will carry away the overloaded electrons (Klinger, 2003).

Regardless of the source of the noise, the end result is an image that needs to be processed. Most post-processing methods include some filtering method to reduce error due to CCD noise. Masks, such as a convolution mask, are typically used to filter the images. The convolution mask uses a matrix technique to determine if a pixel should be as bright as it is in comparison to the pixels around it. The result is a new image that is less sharp to the viewer, but the noise is removed.

CCD alignment. Due to manufacturing limitations, CCD chip alignment will not be identical between cameras. Consider two cameras with printed circuit boards with consecutive serial numbers. During manufacture the CCD chip will be placed on the board on an automated manufacturing line. Machines, such as a Universal Instruments General Surface Mount (GSM) machine, will place the CCD chip onto the board. The GSM has a placement tolerance of plus or minus 55 microns. The pixel size of most quarter inch CCDs is 5.6 microns. If the two boards had CCD chips placed at the extreme opposite tolerance in the x -axis, the difference between the location of the two pixels in relation to coordinate (0, 0) is 110 microns. This would contribute the equivalent of 19 pixels of disparity, and disparity error would be high.

A one-time calibration can be performed to correct this error. To determine this error, one has to place the cameras in a fixture and observe an object in the center that appears near the center of the image at a known distance. Using the error in location, the intrinsic alignment error can be determined.

Distortion. Image distortion is produced by the camera lens aberration. Lens aberration is the result of the light passing through a spherical surface. The light strikes the lens at one angle and leaves at a greater angle. Light striking the lens near the center will have less error than light leaving the edge of the lens. This will result in an image that appears to be distorted around the edges. The further away the scene, the greater the distortion.

Extrinsic camera error. Extrinsic camera error is a concern in stereopsis. Extrinsic error in stereo camera setups is due to the difference in the axis alignment of the two cameras. Disparity error will be greater if the two cameras are not co-planar.

Common narrow-baseline calibrations involve a checkerboard pattern that is observable by both cameras. An algorithm is then used to find the edges of each square. A transformation is then made by an algorithm and post-processes the squares to where it estimates they should be, reducing barrel distortion. This technique is typical for narrow-baseline stereo systems, however for a wide-baseline such as that used in this study a suitable calibration technique did not exist (House and Nickels, 2006)

Barrel distortion is a form of radial aberration “that depends on the distance separating the optical axis from the point of interest” (Forsythe & Ponce, 2003, p. 47). An extreme example of barrel distortion is the fish-eye lens. The outer edges of an image are most affected by barrel distortion.

Stereopsis

Stereopsis used in robotics is similar to stereopsis in humans. An image is projected onto the active CCD matrixes on two different cameras, just as an image is projected onto the retinas of two separate eyes. The difference in location of the object between the two images is used to range an object. To complete this task a robot would use an algorithm in a processing unit, and a human would process this in the brain. The primary difference between stereopsis in robots and in humans is that variables used in the setup of the camera system can be changed, where in humans they are relatively fixed.

Vergence versus parallel images. Human eyes move, and as previously discussed humans use several methods of ranging. Human eyes *fixate* on an object, meaning that the eyes converge inward toward an object. The angles between the center of the lenses of the eyes aligned to the fovea of each eye, and the vertical median symmetry of the head are called *vergence angles* (Forsythe & Ponce, 2003). The closer the object, the more the eyes rotate inward. There are two methods of ranging in stereopsis: vergence and parallel images. This research will be based on the literature of the cameras being *frontal parallel* (Bradski & Kaehler, 2008). Frontal parallel means that the images produced by each of the stereo cameras are assumed to be row-aligned and that every pixel row of one camera is aligned with every corresponding row of the other camera. In the following discussion of disparity range and disparity error, the images will be assumed to frontal parallel.

Disparity range. In relation to Equation 3 and Figure 3, there are four variables that are used to determine the range (r) of an object. The variables are baseline (b), focal

length of the image sensor (f), the pixel size of the sensor (x), and disparity value (N) (Ahuja, 2009; Bradski & Kaehler, 2008).

$$r = bf/Nx \quad (3)$$

Take for example a stereo camera rig with: a baseline of 0.5 meters (m); a 640 x 480 CCD pinhole type camera with a fixed focal length of 2.1×10^{-3} meters and a pixel size of

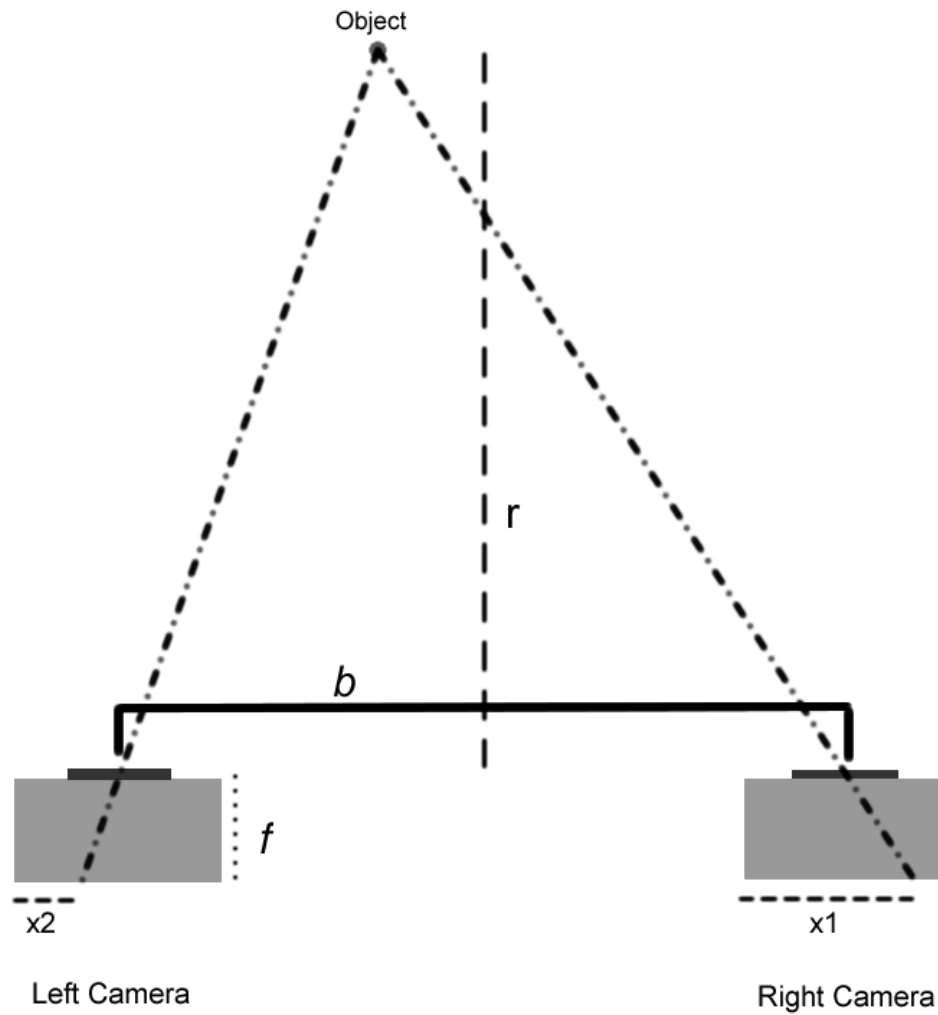


Figure 3. Display of variables for the calculation of disparity range. Copyright 2012 by Kevin Todd Rigby.

5.6×10^{-6} meters; and an object with corresponding pixel centroid (x, y) coordinates of (480, 521) for the left image and (487, 521) for the right image. Using Equation 3, $r = 26.796$ meters. For this and any given setup there is a theoretical minimum and maximum disparity range.

Minimum disparity range. Minimum disparity range (r_{min}) (see Equation 4) is the near blind spot between the two cameras. It depends on the focal length and baseline of the setup. The maximum possible disparity value (N_{max}), is the maximum possible separation on the CCD array in the x -axis, i.e. $N_{max} = 640$ for a 640 x 480 pixel camera.

$$r_{min} = b f / N_{max} x \quad (4)$$

Assuming two pinhole type cameras, such as in the previous example, varying the base will vary the minimum disparity range. Using Equation 4 and a base of 0.5 meters: $r_{min} = 0.2930$ meters. Changing the base to 1 meter: $r_{min} = 0.5860$ meters. Therefore, it can be assumed that increasing the baseline increases r_{min} , and reducing the baseline will reduce r_{min} .

Maximum disparity range. Maximum disparity range (r_{max}) is the point at which an object can move and the movement can still be detected by the CCD array (see Equation 5). The minimum theoretical detectable movement (N_{min}) on the CCD array would be one pixel. If the object is too far away, it will move within the corresponding pixel on each CCD and no change in the (x, y) coordinate will occur.

$$r_{max} = b f / N_{min} x \quad (5)$$

Again, assuming two pinhole type cameras used in the previous examples, varying the base will vary the maximum disparity range. Using Equation 5 and a base of 0.5 meters: $r_{max} = 187.5$ meters. Changing the base to 1 meter: $r_{max} = 375$ meters. Therefore, it can be

assumed that increasing the baseline increases r_{\max} , and reducing the baseline will reduce r_{\max} .

Disparity error. The primary concern for any given stereo setup is the potential disparity error. Disparity error (Δr) is the uncertainty in detecting objects at a particular range. Equation 6 describes the relationship between the actual range (r) of an object and the uncertainty of its position when using stereopsis. For a given stereo setup, the disparity error will change with the change in disparity (ΔN). The change in disparity is in pixels. For the any CCD camera, $\Delta N_{\min} = 1$ (the minimum detectable movement of an object) and for a 640 x 480 pixel camera $\Delta N_{\max} = 640$ (the maximum possible separation on the CCD array).

$$\Delta r = (r^2 / b f) \times \Delta N \quad (6)$$

Using Equation 6, and once again assuming the two pinhole type cameras used in the previous example, a baseline of 0.5 meters, $\Delta N = 1$, and an object at 100 meters, $\Delta r = 53.3$ meters. The uncertainty of locating the object in range would be 100 +/- 53.3 meters. If the same object were at 50 meters away, $\Delta r = 13.3$ meters. Thus, it can be assumed that the further away an object is, the greater the disparity error.

Consider the object at 100 meters in the previous example and an increase in baseline from 0.5 meters to 1.0 meter: $\Delta r = 26.7$ meters. Further increasing the baseline to 2 meters: $\Delta r = 13.3$ meters. Finally, increasing baseline once again to 4 m: $\Delta r = 6.7$ meters. Therefore, it can be assumed that disparity error goes down with an increase in baseline.

Correspondence problem. The problem of a robot knowing whether an object in one image is the same object in the second image of a stereo camera pair, is referred to as

the *correspondence problem*. A normal human looking at an image that includes a basketball, will recognize the object in the image as a basketball without any difficulty. A robot needs an algorithm that is computationally tractable, and also not process intensive to achieve the same level of recognition.

An example of a computationally tractable method used in robotics for identifying common points in images requires the robot to find points of interest that are very light or dark compared to others in the image, or to find well defined edges. Often images are post processed using a thresholding method to transform the image into areas that are all white or black. Images below a certain intensity will be black and images above that level will become white after transformation. This allows the robot to find areas in the map that appear to be the same. Thresholding is used in both monocular and stereoptic systems. Even after thresholding the image, the robot would still have to make some inference as to the object being a basketball which would require another algorithm. What to do with that information goes into an even deeper level in the field of AI.

Chapter Summary

This chapter presented a review of the literature related to human and computer optical sensing. The literature presents a case for the use of a wide-baseline stereo camera system for the detection of in-flight aircraft. The literature also presents the issues of human ranging and sensing as they relate to objects beyond 10 meters. The literature suggests that a wide-baseline stereo camera system may be suitable for the ranging of aircraft as a partial solution to the sense-and-avoid problem. This research contributes to the common body of knowledge in the area of optical sensing, specifically stereo ranging of distant objects.

Chapter III

Method

Introduction

The purpose of this chapter is to present the research design, research questions, hypotheses, variables, procedures, and data collection techniques that were used in this study. The technologies used in this study will also be discussed.

Research Design

The research design used in this study was a quantitative experimental method. The samples were completely self-selected in the sense that the experimenter had no control over the subjects involved in the human ranging pilot study or the aircraft involved in the stereo ranging study.

Samples

Two separate samples were taken for the individual research studies performed. The first set sample data was from human subjects for the human ranging pilot study. The second set of sample data was taken from for the stereo ranging study.

Human ranging pilot study. Human subjects were taken from the random population of students who walked by the experimental area. Aircraft samples were taken from in-flight aircraft within visible range and field of view of the subject.

Stereo ranging study. Samples were taken from in-flight aircraft within a 10

kilometer radius of the Daytona Beach International Airport. The aircraft were aircraft that utilize Automatic Dependent Surveillance-Broadcast (ADS-B). These samples were taken as the aircraft flew within the field of view of the stereo camera rig.

Research Question and Hypothesis

The researcher investigated the following research questions and answered the following hypotheses in this study. Based on the theoretical framework, research questions were created:

1. Can a wide-baseline stereo camera pair range an in-flight aircraft?

Hypothesis 1: A wide-baseline stereo camera pair can range an in-flight aircraft.

2. Can a wide-baseline Axis[®] 207W 640 x 480 pixel stereo camera pair range an in-flight aircraft beyond 4.8 kilometers using a baseline of 14.32 meters?

Hypothesis 2: A wide-baseline 640 x 480 pixel stereo camera pair can range an in-flight aircraft beyond 4.8 kilometers using a baseline of 14.32 meters.

3. Can a wide base-line stereo camera pair range in-flight aircraft more consistently than the sample of humans used in the human localization pilot study?

Hypothesis 3: A wide-baseline stereo camera pair can range an in-flight aircraft more consistently than the sample of humans used in the human ranging pilot study.

Variables

The independent variable in both the human range pilot study and the stereo range study that required precision was that of Global Positioning System (GPS) determined

position of the aircraft. The method of record for the study was that of ADS-B reported position. Embry-Riddle Aeronautical University (ERAU) fleet C-172 aircraft are equipped with identical Garmin G1000 integrated ADS-B glass cockpits.

Human ranging pilot study. There were two independent variables in the human ranging pilot study. The first independent variable was the GPS determined position of the aircraft. The second independent variable was the human subject estimated range of the aircraft.

Dependent variable 1. GPS determined aircraft position was the first independent variable. In this study, GPS position was determined using ADS-B reported data. The ADS-B data was taken from a program developed by the ERAU NEAR Lab that continuously logs ADS-B data. Units of measure were recorded in kilometers and converted to meters for final reporting and analysis.

Dependent variable 2. Human subject estimated range was determined by the subject. Each subject was asked to pick an aircraft visible to them and within their field of view and state the range of the aircraft using the unit of measure of that they felt most comfortable using. All units of measure were converted to meters for reporting and analysis.

Stereo ranging study. There were two independent and one dependent variables in the stereo ranging study. The first independent variable was the location of the aircraft based on GPS coordinates. The second independent variable was the disparity of the aircraft in the x -axis taken from paired stereo images. The dependent variable was disparity range.

Independent variable 1. GPS determined aircraft position was the first

independent variable. In this study, GPS position was determined using ADS-B reported data. The ADS-B data was taken from a program developed by the ERAU NEAR Lab that continuously logs ADS-B data. Units of measure were recorded in kilometers and converted to meters for final reporting and analysis.

Independent variable 2. Disparity in the x -axis was the second independent variable. A stereo camera pair was used to take pictures of in-flight aircraft. The images were uploaded using file transfer protocol (FTP) to a laptop computer. The position of the aircraft in the x -axis were determined for each image. The difference in x -axis pixel location was calculated as disparity.

Dependent Variable. Disparity range was the dependent variable. Disparity range was calculated using Equation 3 for the z -axis.

Procedure

The following procedures outline the experimental setup of the human range pilot study and the stereo range study. Both experiments took place at Embry-Riddle Aeronautical University (ERAU). The experiments took place on two separate days under similar meteorological conditions.

Human ranging pilot study. Only ADS-B reporting aircraft were included in the study. To ensure consistency, only ERAU ADS-B equipped Cessna 172 fleet aircraft were included in the data.

Location setup. A table was set up in an area with high student traffic. The area had a 360 degree lateral view of the sky and between 3 and 30 degrees vertical view in reference to the horizon.

Data collection. Two sources of data were recorded in this study, ADS-B data

and subject reported data. The ADS-B data was recorded on an ERAU server. The data was provided to the researcher in a comma separated variable (CSV) format. The subject reported data was hand recorded.

Subject reported data. Subjects verbally announced the estimated range of an aircraft. The subject estimated range was then recorded along with time, researcher estimated range, researcher estimated altitude, and magnetic bearing to the aircraft. Magnetic bearing was determined using a lensatic compass.

ADS-B data. The ERAU ADS-B database was queried for ADS-B data for the time duration of the experiment. The researcher filtered the data to a radius of 15 kilometers. The researcher was then able to identify the aircraft in the images based on time, bearing, and altitude when compared to the recorded subject data.

Stereo range study. Only ADS-B reporting aircraft were included in the study. To ensure consistency, only ERAU ADS-B equipped Cessna C-172 fleet aircraft were included in the data.

Camera setup. The camera rig was set up on the roof of the College of Aviation building at ERAU. Two Axis® 207W 640 x 480 pixel CCD network cameras were placed on a southward facing ledge of the building 14.32 meters apart. The location of the center point between the two cameras was recorded using GPS. The two cameras were connected to a Netgear® router using two 10 meter Cat-5 Ethernet cables. The router was connected to a laptop to form a local area network. File transfer protocol (FTP) was used to transfer images from the cameras to the laptop which ran a local FTP server. Figure 4 is a photo of the actual stereo camera set-up used on the day the research data was collected.



Figure 4. Stereo camera set-up used in the research study. Copyright 2012 by Kevin Todd Rigby.

Camera calibration. The camera error was determined using known points in the visual field. The known GPS position of radio towers, buildings, and fixed objects was used to determine the disparity error of the camera at varying distances and angles within the field of view.

Camera alignment. Narrow-baseline cameras are normally aligned on a fixture. The alignment process for narrow base cameras is performed as a one-time alignment, normally at the manufacturing facility. Due to the nature of the wide baseline, this research study required that the alignment be performed in the field.

Camera alignment in this study was performed mechanically. Each Axis[®] 207W

camera had two alignment plates attached to it. The first plate was attached to the back of each camera with two fixed line levels. The line levels aligned the cameras in the x , y -axes. Magnetic compasses were attached to the top plate (see Figure 5).



Figure 5. Initial camera alignment method. Copyright 2012 by Kevin Todd Rigby.

Variation between the two compasses was verified using a fixture that was used to take images of a fixed target cross-hair (See Figure 6). Magnetic variation was marked on each compass. The method of mechanical alignment was verified on a narrow baseline using the fixture.

The fixtures were used to initially align the cameras in the x , y -axes on the roof. A known point on the ground was used to determine the disparity in pixels at the range of the departing aircraft. Images were taken using the two Axis[®] 207W cameras, and using

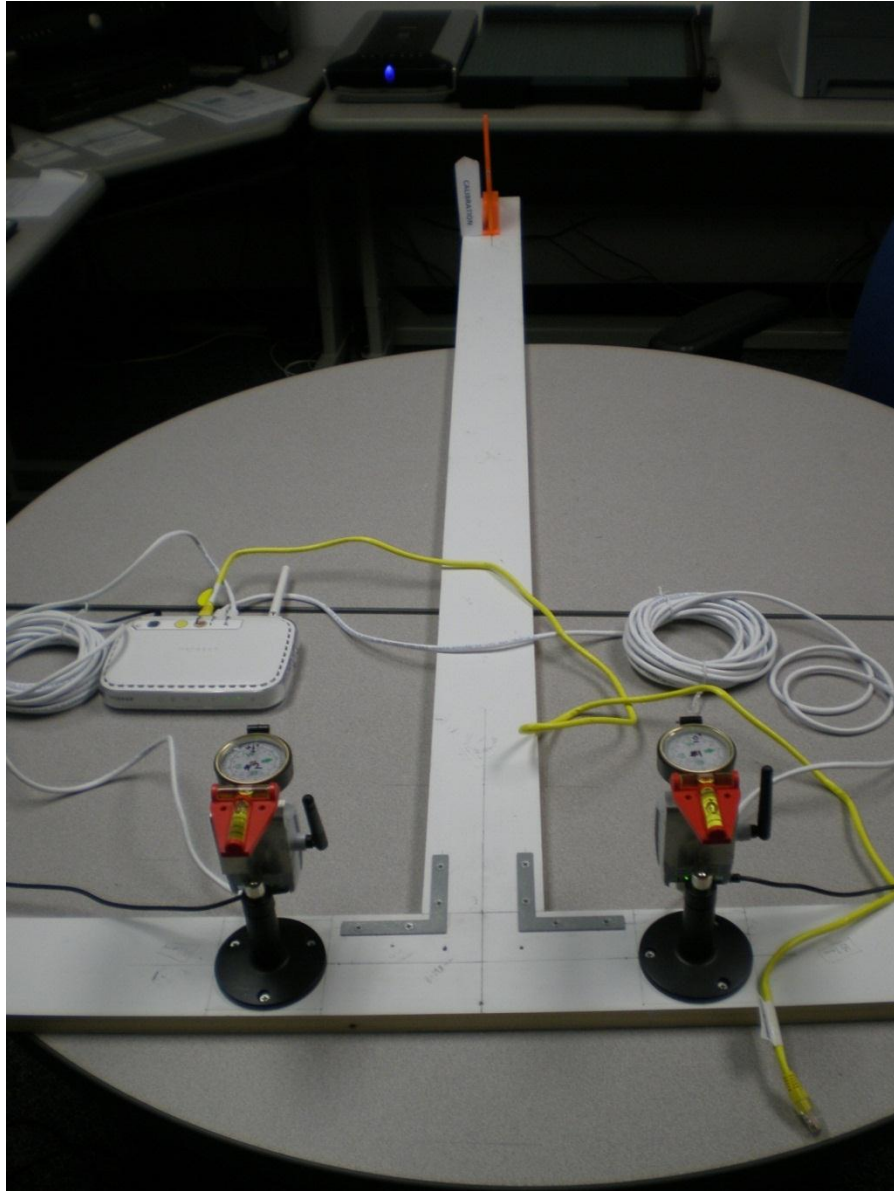


Figure 6. Manual calibration verification fixture. Copyright 2012 by Kevin Todd Rigby.

ImageJ the point in the left image was located. The left camera was adjusted until the point in the left image was where it should be in terms of disparity. The images were aligned to within one pixel in both the x and y axis. This method of calibration addressed both intrinsic and extrinsic calibration. The one pixel error was corrected in the post processing calculations.

Data collection. Two sources of data were recorded in this study, ADS-B data

and stereo camera images. The ADS-B data was recorded on an ERAU server. The data was provided to the researcher in a CSV format. The stereo images from the cameras were uploaded to a laptop via local FTP.

ADS-B data. The ERAU ADS-B database was queried for ADS-B data for the time duration of the experiment. The researcher filtered the data to a radius of 10 kilometers for bearings 080 degrees to 180 degrees magnetic. The researcher was then able to match the aircraft in the ADS-B database based on time, bearing, and altitude to aircraft in the image data set.

Stereo camera data. When an aircraft appeared within a suitable field of view, the stereo cameras were activated manually using the software program supplied by Axis[®]. The software allows for a camera timestamp to be synchronized to the laptop clock. The camera synchronization was tested using a digital watch. Images were recorded of the digital watch in stopwatch mode. The camera recording rate was set to 10 Hz. The smallest interval that the stopwatch reports is 1/100 seconds. Five image pairs of the stopwatch were analyzed and at identical times on the stopwatch the timestamps on the image pairs were within 20/100 seconds. Synchronization of the cameras was determined in post processing by using vehicles in the visual field and aligning them at a given point on the ground, and then determining the time synchronization of the cameras. It was determined that there was a 2.1 second difference in time stamps on the two cameras throughout the entire experiment. Image pairs were matched based on this time difference. Figure 7 is a stereo image-pair from dataset 4.

Data analysis. Post-process data analysis was performed on the raw ADS-B data and the stereo image pairs. The ADS-B data was processed using Microsoft[®] Excel. The



Figure 7. Example stereo dataset. Copyright 2012 by Kevin Todd Rigby.

stereo camera image pairs were processed using *ImageJ*, a Java™ image processing and analysis application. The data obtained from the image was processed in Microsoft® Excel.

ADS-B data analysis. The raw ADS-B data of interest was recorded as latitude and longitude in decimal form. The latitude and longitude data were used to determine distance and bearing to an aircraft from the base location of the camera rig, specifically the center point between the two cameras. Distance was calculated using the Law of Spherical Cosines (Veness, 2010). The ADS-B data was used to match the proper aircraft using the time, bearing, and distance.

Stereo image pair analysis. The stereo image pairs were analyzed separately using *ImageJ*. The x -axis centroid of the aircraft in each image was determined manually by the researcher using the darkest pixel of the aircraft. The disparity range was calculated using the disparity of the two images in terms of the pixel distance between the centroid of the aircraft in the left and right image of each pair.

Hypothesis 1 analysis. The qualitative data for H1 was analyzed subjectively. H1 will be accepted if the system detects and ranges an aircraft regardless of error.

Hypothesis 2 analysis. The quantitative data for H2 was analyzed. H2 will be accepted if the system detects and ranges an in-flight aircraft beyond 4.8 kilometers regardless of error.

Hypothesis 3 analysis. The quantitative data for H3 was analyzed using the statistical analysis unpaired t-test. H3 will be accepted at $p < 0.001$.

Chapter Summary

The purpose of this study was to investigate the efficacy of using wide-baseline stereopsis to range aircraft. This chapter provided the research questions and related hypotheses, variables, and method for the study. It also details the software and data collection techniques and procedures.

Chapter 4

Results

Introduction

In this research study, stereopsis was used as a method to range aircraft in the z -axis. A wide-baseline of 14.32 meters was used to examine the efficacy of this method of ranging. The results from this study are presented in this chapter. The research questions are first discussed, followed by the data, and finally the data analysis.

Research Questions

Based on the theoretical framework, three research questions were developed:

1. Can a wide-baseline stereo camera pair range an in-flight aircraft?
2. Can a wide-baseline Axis[®] 207W 640 x 480 pixel stereo camera pair range an in-flight aircraft beyond 4.8 kilometers using a baseline of 14.32 meters?
3. Can a wide-baseline stereo camera pair range in-flight aircraft more consistently than the sample of humans used in the human ranging pilot study?

Ranging Results

The wide-baseline ranging of aircraft indicated that the system was capable of ranging aircraft. The ranged position of the aircraft in the data-group, with the exception of one, were all on the near side of the flight path of the aircraft. The near side means that

the ranges were biased toward being closer than actual.

Human ranging pilot study. A total of 31 subjects participated in the human ranging pilot study. Seven of the aircraft targets did not have ADS-B onboard, so seven of the data points were not usable. Therefore, a total of 24 data points were analyzed. There were two extreme outliers that were outside of two standard deviations. The outliers were removed from the data leaving 22 total data points that are included in the analysis of the ranging study. The aircraft ADS-B positions ranged from 650.6 meters to 9,738.3 meters. The subjects' estimations ranged varied from 24 to 11,265 meters. The absolute percent error was calculated for each pairing between the ADS-B position and the estimated range. The mean absolute percent error was 50.34%. Appendix C presents the post-processed human ranging pilot study data.

Table 1

Human Ranging Pilot Study Descriptive Data

Data Type	ADS-B Position	Subject Estimated Range
<i>n</i>	22	22
Mean	3406.3 m	1691.7 m
Standard Deviation	2780.6 m	2504.5 m
High	9738.3 m	11265.0 m
Low	650.6 m	24.0 m

Stereo study data. A total of 51 image and ADS-B data sets were taken using the method described in Chapter 3. Out of the 51 sets, 17 sets were usable. Appendix A presents examples of these image pairs. The criteria for the use of data in the analysis and reporting of results was simple; the aircraft must be visible and identifiable in both

images and ADS-B data must exist for the aircraft in the two images. Appendix B summarizes the acceptance criteria of data for each aircraft.

The ADS-B position of the aircraft ranged from 825.48 meters to 990.51 meters. The wide-baseline stereo calculated range varied from 603.13 to 855.15. The mean absolute percent error between the ADS-B position and the stereo ranged position of the aircraft was 17.62%. Appendix D presents the post-processed stereo ranging study data.

Table 2

Wide-based Stereo Descriptive Data

Data Type	ADS-B Position	Stereo Estimated Range
N	17	17
Mean	905.51 m	745.94 m
Standard Deviation	44.35 m	75.21 m
High	990.51 m	855.15 m
Low	825.48 m	603.13 m

Data Analysis

In this study, the researcher addressed Research Question 1, Research Question 2, and Research Question 3 and tested for any significant difference in the means of the human range pilot study and the wide-baseline stereo ranging method. An Unpaired *t*-test was used to address Research Question 3.

Research question 1. Can a wide-baseline stereo camera pair range an in-flight aircraft? The wide-baseline stereo camera system was able to range in-flight aircraft with a 17.63% error in position in the *x*-axis.

Research question 2. Can a wide-baseline Axis® 207W 640 x 480 pixel stereo

camera pair range an in-flight aircraft beyond 4.8 kilometers using a baseline of 14.32 meters? Several aircraft were selected at a range beyond 1 kilometer, however no visible aircraft could be detected in any of those images.

Research question 3. Can a wide-baseline stereo camera pair range in-flight aircraft more consistently than the sample of humans used in the human ranging pilot study? The null hypothesis was that there is no significant difference between human range estimation and the wide-baseline stereo camera ranging method used in this study.

The mean absolute percent error for the human subjects was 50.3% and the mean absolute percent error for the wide-baseline stereo camera system was 17.6%. An unpaired *t*-test was performed. There was a significant difference in the absolute percent error of the human subjects ($M=63.64$, $SD=30.44$) and the wide base-line stereo system error ($M=17.64$, $SD=8.89$); $t(37)=2.887$, $p=0.000$. These results suggest that the wide-baseline stereo camera system is more consistent as well as more accurate than humans at ranging in-flight aircraft.

Chapter Summary

The descriptive statistics and statistical test were presented in this chapter. The focus of this research study was to determine the efficacy of a wide-baseline stereo camera system for the ranging of aircraft. The study answered Research Question 1 and was able to range an in-flight aircraft. For Research Question 2, the cameras used in this study were not able to detect aircraft beyond one kilometer. Finally, Research Question 3 was answered and the results suggest that the wide-baseline stereo camera system was able to range in-flight aircraft more consistently and accurately than humans. Discussion of these results and interpretations are presented in Chapter 5.

Chapter V

Conclusions

Introduction

The purpose of this study was to examine the efficacy of using wide-baseline stereopsis as a method for the ranging of in-flight aircraft. The capability to range, range within a given distance, and the comparison to human ranging was of interest to the researcher.

Study Summary

A wide-baseline stereo camera system was setup on the top of the three-story College of Aviation building at Embry-Riddle Aeronautical University (ERAU) with a wide unobstructed field of view of two departing runways 7L and 7R. An experimental method was used where 17 total usable stereo image pairs were obtained over a period of 4 hours. Automated Dependent Surveillance Broadcast (ADS-B) data was collected for each aircraft and position was matched to the time synch of the World Clock time used on the laptop and cameras. The stereo images were used to determine the range to the aircraft in the x -axis. The ranged of the ADS-B position and the stereo ranged position were then compared using a percent error method. The results of the study were positive.

Results

The wide-baseline stereo system was able to range in-flight aircraft. The system

Ranged aircraft more consistently and more accurately than human subjects that were tasked with ranging of in-flight aircraft in a pilot study conducted by the researcher.

The difference in variability in the range of the aircraft in the human ranging pilot study was much higher than that of the wide-baseline stereo ranging study. This was not something that could be controlled by the researcher. Aircraft visible to the naked eye were selected and the field of view in which they flew was recorded, but due to the limitation of the Axis[®] 207W cameras, those aircraft were not identifiable in any of the images. Therefore, the difference in variability existed.

Research question 1. Can a wide-baseline stereo camera pair range an in-flight aircraft? A wide-baseline stereo camera pair can range an in-flight aircraft. The null hypothesis that a wide-baseline stereo camera pair cannot range an in-flight aircraft was rejected.

Research question 2. Can a wide-baseline Axis[®] 207W 640 x 480 pixel stereo camera pair range an in-flight aircraft beyond 4.8 kilometers using a baseline of 14.32 meters? The cameras were not able to detect any aircraft in the visual field beyond one kilometer. The null hypothesis that a wide-baseline 640x480 pixel stereo camera pair cannot range an in-flight aircraft beyond 4.8 kilometers using a baseline of 14.32 meters was accepted.

Research question 3. Can a wide-baseline stereo camera pair range in-flight aircraft more consistently than the sample of humans used in the human ranging pilot study? A wide-baseline stereo camera system can range in-flight aircraft more consistently and accurately than humans. The null hypothesis that a wide-baseline stereo camera system cannot range in-flight aircraft more consistently than humans used in the

human ranging pilot study was rejected.

Discussion

Wide-baseline stereopsis presented a method for the ranging of aircraft. The research presented here suggests that it is one possible solution to the ranging of aircraft.

Research question 1. The data for Research Question one is a simple quantitative answer, the aircraft was present in the stereo image pair and a ranged position in the x -axis was determined. The data had positional error and all but one position were biased toward the near side of the aircraft's flight path.

Research question 2. The data for Research Question 2 did not present evidence that the Axis[®] 207W 640x480 pixel camera could range an aircraft at 4.8 kilometers. The cameras did not detect any aircraft beyond one kilometer.

Research question 3. The data for Research Question 3 suggest that a wide-baseline stereo camera system does have the capability to range aircraft more consistently and accurately than the human sample in the human ranging pilot study.

Implications of the Study

The literature review, data analysis, and interpretation of the results have been discussed and several implications are clear. The first implication is that a wide-baseline stereo camera system could be a core technology in the sense-and-avoid problem. There are numerous low radar signature aircraft that may not be recognized by radar as primary targets. The wide-baseline stereo system can detect these aircraft. Another implication is that of the detection of birds. The study focused on aircraft, but birds can be considered low signature targets that pose risk to in-flight aircraft. With a high enough camera charge coupled device (CCD) density tertiary targets such as birds may be detected and

ranged.

Recommendations for Future Research

Recommendations for this study include the use of aircraft capable of logging Global Positioning System (GPS) position, higher resolution cameras, a better time synchronization system for the cameras, the study of bird sized targets, multiple sessions under various conditions, the use of multiple types and sizes of aircraft, the use of infrared cameras, develop a post-process transformation technique for the elimination of barrel distortion and thresholding the aircraft in the image, a scale expansion of the ranging pilot study, and a the use of a better camera positioning system.

1. Replicate the study using Cessna 172 aircraft equipped with the Garmin FDM capable of logging the GPS position of the aircraft at 10hz.
2. Replicate the study using higher resolution cameras to determine the resolution needed to detect aircraft up to 4.8 kilometers.
3. Replicate the study with CCD cameras that can be triggered for synchronized static photos and independent image integration.
4. Replicate the study with bird sized targets that can data-log GPS position.
5. Replicate the study under varying meteorological conditions.
6. Replicate the study using at least three different types and sizes of aircraft.
7. Replicate the study using infrared cameras under varying conditions.
8. Develop a post-process transformation technique for the elimination of barrel distortion and thresholding of the aircraft.
9. Perform a scale version of the human ranging study to include localization.
10. Study the localization of aircraft using present and future wide-baseline stereopsis

data.

11. Replicate the study using a better camera positioning system that can align the cameras using servos.

Limitations of the Study

There were four limitations to the study. The first was the lack of a suitable stereo calibration technique for wide-baseline stereo camera systems. Barrel distortion is the primary source of error in this situation. This would have led to a greater positional error for aircraft on the outer edges of the images. Due to this problem, only aircraft centered in the inner quartile of the CCD array were used from each data set. Data sets included numerous images of each aircraft, so the researcher could select aircraft data sets in such a way.

The second limitation was that of the ADS-B update being limited to 1 hertz. The update rate of the CCD cameras was 10 hertz. Considering integration time, the difference between a matched stereo pair and the aircraft position was not completely synchronized.

The third limitation was that of camera resolution. The Axis[®] 207W 640x480 pixel camera was not able to detect aircraft out beyond one kilometer. This is most likely due to the optical quality of the lens and focal length.

The fourth limitation to the study was that each image was manually analyzed and the centroid of the aircraft was considered to be the one that appeared to be darkest. This is a subjective determination based on the researcher's interpretation.

Aircraft Deployment

The potential exists for aircraft deployment of the core technology. A qualified

engineer would have to determine that the chosen cameras would not cause bending moment or flutter problems. Assuming that it would be safe to deploy the system, two cameras would be fixed to the wing tips of an experimental aircraft.

Several factors must be considered, in terms of image alignment, when the aircraft takes flight. Aerodynamic factors include but are not limited to wing twist, bending moment, and vibration. Any of the three factors listed would cause the images to no longer be frontal parallel. To correct for these factors a method of inertial measurement of the independent position of each camera in reference to the other would have to be developed. Once independent position is determined, an image could then be translated to frontal parallel equivalence. Finally, after image translation occurs, the system could then begin to identify aircraft within the visual field using a search algorithm. Range could then be determined to any identified aircraft.

Chapter Summary

The main purpose of this study was to determine the efficacy of wide-baseline stereopsis for the ranging of in-flight aircraft. This chapter provided a discussion of the results, implications, recommendations, and limitations of the study. The results provide data that suggests that wide-baseline stereopsis has efficacy in the ranging of in-flight aircraft. Implications are that with future research, the core technology may be suitable as part of a sense-and-avoid solution. Recommendations were made for future research using differing and higher quality technologies, research under varying meteorological conditions, different types of aircraft, the development of a suitable calibration technique, and a full-scale human ranging and localization study. Further research is needed to determine the application and deployment of wide-baseline stereopsis.

References

- Ahuja, S. (2009). *How to select a proper disparity value for stereo-vision*. Retrieved November 25, 2009, from Wordpress.com Web site:
<http://siddhantahuja.wordpress.com/2009/7/24/hot-to-select-the-proper-disparity-value-for-stereo-vision/>
- Anvari, M., McKinley, C., & Stein, H. (2005). Establishment of the world's first telerobotic remote surgical service for provision of advanced laparoscopic surgery in a rural community. *Annals of Surgery*, 241(5), 460-464.
doi:10.1097/01sla.0000154456.69815.ee
- Asimov, I., & Frenkel, K.A., (1985). *Robots*. New York, NY: Harmony Books.
- Blake, R., & Sekuler, R. (2006). *Perception* (5th ed.). New York, NY: McGrawHill.
- Blehm, C., Vishnu, S, Khattak, A., Mitra, S., & Yee, R. W. (2005). Computer vision syndrome: a review. *Survey of Ophthalmology*, 50(3), 253-262.
doi:10.1016/j.survophthal.2005.02.008
- Bradski, G., & Kaehler, A. (2008). *Learning OpenCV*. Sebastopol, CA: O'Reilly Media Inc.
- Davis, J.R., Johnson, J., Stepanek, J., & Fogarty, J.A. (Eds.). (2008). *Fundamentals of Aerospace Medicine* (4th ed.). Philadelphia, PA: Lippincott Williams & Wilkins.

- Dehart, R.L. (Ed.). (1985). *Fundamentals of Aerospace Medicine*. Philadelphia, PA: Lea & Febiger.
- Dehart, R.L., & Davis, J.R. (Eds.). (2002). *Fundamentals of Aerospace Medicine*. (3rd ed.). Philadelphia, PA: Lippincott Williams & Wilkins.
- Federal Aviation Administration. (2008). *Interim Operational Approval Guidance 08-01*. Washington, DC: Author.
- Federal Aviation Administration. (2010). *Federal Aviation Regulations (Part 67)*. Washington, DC: Author,
- Forsythe, D.A., & Ponce, J., (2003). *Computer vision: a modern approach*. Upper Saddle River, NJ: Prentice Hall.
- Gibb, R., Gray, R., & Scharff, L. (2010). *Aviation Visual Perception*. Burlington, VT: Ashgate Publishing Company.
- Goldstein, E.B., (1999). *Sensation and perception* (5th ed.). Pacific Grove, CA: Brooks/Cole Publishing Company.
- Hibbard, P.B. (2008). Binocular energy responses to natural images. *Vision Research*, 48(1), 1427-1439.
- House, B., & Nickels, K. (2006). Increased automation in stereo camera calibration techniques. *Journal of Systemics, Cybernetics and Informatics* 4(4), 48-51.
- Klinger, T., (2003). *Image processing with labview IMAQ vision*. Upper Saddle River, NJ: Pearson Education, Inc.
- Liebowitz, H. W. (1988), The human senses in Flight. In E. L. Wiener & D.C. Naagel (Eds), *Human factors in aviation* (pp. 83-110). New York, NY: Academic Press.

- Murphy, R.R., (2000). *Introduction to AI robotics*. Cambridge, MA: The MIT Press.
- Niku, S.B. (2001). *Introduction to Robotics, Analysis, Systems, Applications*. Upper Saddle River, NJ: Prentice Hall.
- Reinhardt, R.O., (2008). *Basic Flight Physiology*. New York, NY: McGrawHill.
- Roble, D. (2005). Computer vision in visual effects. In G. Medioni & S. B. Kang (Eds.), *Emerging topics in computer vision* (pp. 306-332). Upper Saddle River, NJ: Prentice Hall.
- Shan, J., & Sampath, A. (2007). Urban terrain and building extraction from airborne LIDAR data. In Q. Weng & D. A. Quattrochi (Eds.), *Urban remote sensing* (pp. 21-45). Boca Raton, FL: CRC Press.
- Veness, C. (2010). *Calculate distance, bearing, and more between latitude/longitude points*. Retrieved February 6, 2011, from <http://www.movable-type.co.uk/scripts/latlong.html>

Appendix

Appendix A

Examples of Aircraft Image Pairs

Set 4



Set 6



Appendix B
File Usage Evaluation Criteria

File Usage Evaluation Criteria

File #	Criteria	File#	Criteria
1	No image match	27	Good
2	No AC	28	No AC
3	No AC	29	Good
4	Good	30	No image match
5	Good	31	No image match
6	Good	32	No AC
7	No image match	33	Good
8	Good	34	No AC
9	No image match	35	Good
10	Good	36	No AC
11	No AC	37	No image match
12	No image match	38	No ADS-B
13	Good	39	No ADS-B
14	Good	40	No image match
15	No AC	41	No image match
16	Good	42	No image match
17	No AC	43	No AC
18	No AC	44	No ADS-B
19	No AC	45	Good
20	No AC	46	No AC
21	Good	47	No image match
22	Good	48	No AC
23	No AC	49	No ADS-B
24	No AC	50	No AC
25	Good	51	No ADS-B
26	Good		

Appendix C

Human Ranging Pilot Study Data

Human Ranging Pilot Study Data

Set	Target Address	Meters ADS-B	Bearing ADS-B	Time ADS-B	EST Time	EST Bearing	Est Meters	%Error	% Error Absol
1	10845621	650.57	25.65	18.8598329	18.879	30	400	-38.515	38.515
2	10779949	865.30	54.27	19.45060981	19.46	40	610	-29.504	29.504
3	10832657	925.62	163.63	19.03388889	19.036	150	244	-73.639	73.639
4	11098297	938.23	156.00	19.10411024	19.108	140	1931	105.814	105.814
5	11112212	1056.01	68.97	18.91838759	18.922	60	300	-71.591	71.591
6	10854781	1154.66	135.17	19.5996658	19.604	160	644	-44.226	44.226
7	10886065	1467.70	108.99	18.35688802	18.367	100	402	-72.610	72.610
8	10888918	1758.29	100.02	18.58272135	18.588	130	100	-94.313	94.313
9	11109359	1784.23	99.32	19.34210938	19.347	100	2414	35.297	35.297
10	11098297	2036.71	175.70	19.27333333	19.246	160	1207	-40.738	40.738
11	11098297	2077.47	103.63	19.1146658	19.119	110	4023	93.649	93.649
12	11098297	2127.90	101.72	19.32866536	19.3	140	600	-71.803	71.803
13	10761279	2441.08	110.13	18.4573329	18.479	123	1979	-18.929	18.929
14	10761279	3238.57	153.92	18.3818316	18.4	160	4023	24.221	24.221
15	10834559	3414.68	152.05	18.98294271	19	140	549	-83.922	83.922
16	10863941	4885.51	10.27	19.29405382	19.297	10	4023	-17.654	17.654
17	10832657	5378.40	97.92	19.07116536	19.092	70	305	-94.329	94.329
18	10852879	6331.40	102.84	18.68255425	18.683	120	1200	-81.047	81.047
19	11109359	6521.37	149.54	19.3971658	19.404	140	61	-99.065	99.065
20	10832657	7039.47	103.01	19.08399957	19.097	100	914	-87.016	87.016
21	10501486	9107.41	246.76	19.42861111	19.433	210	11265	23.690	23.690
22	11404308	9738.26	170.65	19.01822483	19.008	170	24	-99.754	99.754

Appendix D
Stereo Ranging Study Data

Stereo Ranging Study Data

Image Folder	Bearing	Time ADS-B	Time Cam	D Ave ADS-B	D Stereo	%Error	%Error Abs
4	135.97	16.46377604	16.463961	838.156	855.146	2.027	2.027
5	133.52	16.56622179	16.5663194	897.876	728.336	-18.882	18.882
6	130.42	16.60338759	16.603583	974.494	774.264	-20.547	20.547
8	138.49	16.68666667	16.6869	911.041	774.264	-15.013	15.013
10	134.70	16.75227648	16.752492	908.713	750.601	-17.400	17.400
13	141.63	16.85755425	16.857611	825.481	707.359	-14.309	14.309
14	133.52	16.91149957	16.911622	895.538	799.466	-10.728	10.728
16	140.88	16.97294271	16.973058	863.444	651.098	-24.593	24.593
21	137.09	17.13372179	17.13385	906.047	774.264	-14.545	14.545
22	132.53	17.16972222	17.169881	884.299	687.557	-22.248	22.248
25	129.82	17.27027778	17.270381	953.993	707.359	-25.853	25.853
26	150.10	17.30644314	17.306522	877.737	855.146	-2.574	2.574
27	125.61	17.5843316	17.584369	955.345	855.146	-10.488	10.488
29	131.20	17.69055556	17.690833	990.508	707.359	-28.586	28.586
33	129.76	18.12994358	18.1299	900.016	799.466	-11.172	11.172
35	130.81	18.33511068	18.335272	917.930	603.127	-34.295	34.295
45	131.20	18.93099826	18.9312861	887.014	651.098	-26.597	26.597